

## Solitary Modes and the Eckhaus Instability in Directional Solidification

Adam J. Simon, John Bechhoefer, and Albert Libchaber

*Department of Physics and The James Franck and Enrico Fermi Institutes,  
The University of Chicago, 5640 S. Ellis Avenue, Chicago, Illinois 60637*

(Received 7 July 1988)

In a directional solidification experiment on a moving nematic-isotropic interface, we observe solitary modes propagating across the interface. We also observe the Eckhaus instability. In the presence of solitary modes, the pattern-selection mechanism is dynamic.

PACS numbers: 68.10.La, 61.30.Jf

In a previous study,<sup>1</sup> we reported observations of the Mullins-Sekerka instability<sup>2-4</sup> of a moving nematic-isotropic interface of thin, slightly impure liquid crystal.<sup>5</sup> As a function of the interface velocity  $v$ , we observed three regimes. For velocities less than a critical velocity  $v_c$ , the interface is flat. For  $v_c < v < v_d$ , the interface is cellular, almost periodic and stationary in the reference frame moving at the front velocity  $v$ . Above a second critical velocity  $v_d$ , the interface leaves a series of droplets of the isotropic phase behind.

In the experiments we report here, we show that in the cellular regime ( $v_c < v < v_d$ ), one observes solitary modes that propagate along the interface, transverse to the overall direction of interface motion. As discussed below, solitary mode motion is closely linked to a unique wavelength selection.<sup>6</sup>

We also show that by first increasing the interface velocity to  $v \gg v_d$  and then reducing  $v$  to a value in the cellular regime, we can impose a smaller cell wavelength. If the contrast in wavelength is large enough, we observe period doubling of the cellular pattern, or occasionally, a larger period multiple. When the contrast in wavelengths is still larger, the interface undergoes a series of increasingly large-amplitude fluctuations that terminate in the destruction of one or more cells, and hence in an increase in wavelength of the cells that remain. We believe these fluctuations to be a manifestation of the Eckhaus instability,<sup>7,8</sup> which has been observed in other systems.<sup>9,10</sup>

Our samples consist of two parallel glass plates (bottom plate,  $24 \times 28 \times 1$  mm<sup>3</sup>; top plate  $22 \times 22 \times 1$  mm<sup>3</sup>) separated by a wire spacer to a gap of  $26.5 \pm 1.5$   $\mu$ m. The gap is filled by capillary action with the liquid crystal 4-*n*-octylcyanobiphenyl (8CB) doped with 1.2 mol% hexachloroethane. 8CB is chosen for its chemical stability and its convenient nematic-isotropic transition temperature (40.5°C). The inner glass surfaces of the sample were treated with silane<sup>11</sup> to orient the nematic phase perpendicular to the glass plates, a configuration known as homeotropic.

Our directional solidification apparatus is standard<sup>12</sup> and will be described elsewhere.<sup>13</sup> Briefly, one end of the sample is placed in a hot oven and the other end in a cold

one, separated by a 4-mm gap. The high thermal conductance of the glass plates imposes a linear temperature gradient along the sample. The temperatures are chosen so that the nematic-isotropic interface sits in the gap, where it is observed in bright-field microscopy. The experiment consists of moving the sample at a controlled velocity from the hot side to the cold side, while holding the ovens fixed. Thus, we "freeze" the liquid, creating the nematic phase at constant rate.

In our sample, we measured an onset velocity  $v_c$  of  $v_c = 16.0 \pm 0.5$   $\mu$ m/sec at a temperature gradient of  $23 \pm 1$  K/cm. At onset, the critical wavelength  $\lambda_c$  is  $96 \pm 7$   $\mu$ m. The dispersion in  $\lambda_c$  is due mostly to the variation of the cells themselves rather than to the precision of our measurements ( $\pm 2$   $\mu$ m).

For  $16 < v < 38$   $\mu$ m/sec, we observe cells whose amplitude increases and wavelength decreases with velocity. In this regime, there is approximately a 5% scatter in the cell wavelength at any given velocity. As we increase the velocity, the wavelength is decreased via tip splitting.

At a critical velocity  $v_s = 38$   $\mu$ m/sec, a new regime appears with defect motion. These defects, which we call solitary modes, propagate in both directions along the interface. The solitary mode is a region of the interface where cells are stretched to connect two regions of "normal"-sized background cells. We call the defects solitary modes rather than fronts<sup>14</sup> because two stable states are connected. Figure 1 shows a complete cycle of the solitary mode's motion: A background cell in front (i.e., to the left in the photo) of the solitary mode is stretched at the same time the last piece of the solitary mode is compressed to form a new normal cell. Although the sequence of solitary mode shapes is representative, not all solitary modes show the same amount of stretching. They can also vary in length, from one to ten stretched domains. A stretched domain can extend to almost the length of two background cells.

Solitary mode velocities show scatter. At  $v = 40$   $\mu$ m/sec, we measured solitary mode velocities of 16 to 33  $\mu$ m/sec, with most measurements in the range 25–28  $\mu$ m/sec. At  $v = 48$   $\mu$ m/sec, we measure velocities of 28–38  $\mu$ m/sec, with the average clustering around 30 to 31  $\mu$ m/sec. Roughly, one can say that the solitary modes

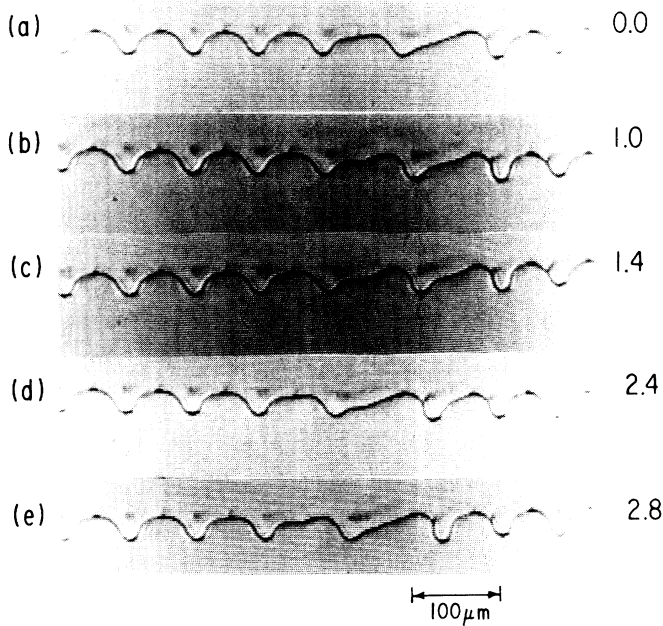


FIG. 1. Solitary mode propagating to the left. The sequence shows one cycle of the motion, with the time indicated, in seconds, on the right. Interface velocity = 40  $\mu\text{m}/\text{sec}$ .

travel at approximately  $\frac{2}{3}$  the front velocity. Larger solitary modes tend to travel faster: A tripling of solitary mode length changes the velocity by about 10%. The main reasons for the scatter are the effects of perturbations of the interface due to dust particles and defects in the silane treatment of the glass. Both these effects can change a solitary mode's length, split it in two, or even destroy it.

If a right-moving solitary mode meets a left-moving solitary mode of equal length, the two annihilate each other. Thus, the solitary modes are dissipative, rather than dispersive. More generally, if a solitary mode of length  $l$  meets a smaller solitary mode of length  $l'$ , the result is a solitary mode of length  $l - l'$  moving in the direction of  $l$  (Fig. 2). The solitary mode is stable to small perturbations. We have seen solitary modes that propagate across the entire 2-cm sample (300 cells).

A most remarkable feature of the solitary modes is their effect on wavelength selection. When the velocity is changed suddenly from zero to a velocity in the range where solitary modes are observed, the initial pattern contains many wavelengths. After the passage of just one solitary mode, the average value of the wavelength is reduced and has a much more uniform distribution (Fig. 3). As the solitary mode moves through a field of background cells, it packs the trailing cells to a uniform spacing  $\lambda_s$  behind it. Further solitary modes, in either direction, do not affect the value of the wavelength. When the states before and after the solitary mode have different wavelengths, the phase slip between the two

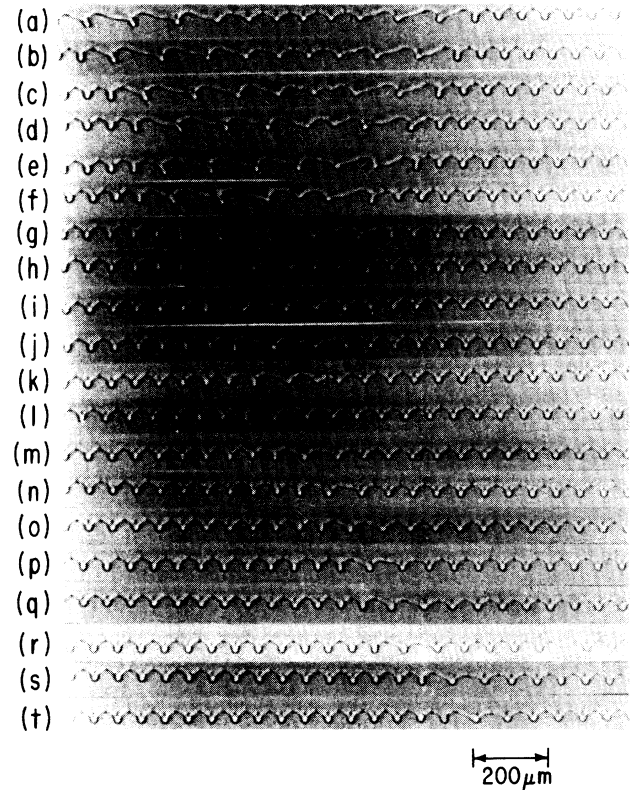


FIG. 2. Collision of two solitary modes. The result of the collision will be a single solitary mode propagating to the right. Velocity = 40  $\mu\text{m}/\text{sec}$ .

states accumulates. Eventually, either a new stretched domain will form or a new normal cell will be inserted.

We have seen that a solitary mode will compress large cells to some selected wavelength  $\lambda_s$ . What if we start with a wavelength smaller than  $\lambda_s$ ? Starting at a high velocity (100  $\mu\text{m}/\text{sec}$ ) and then quickly reducing to a ve-

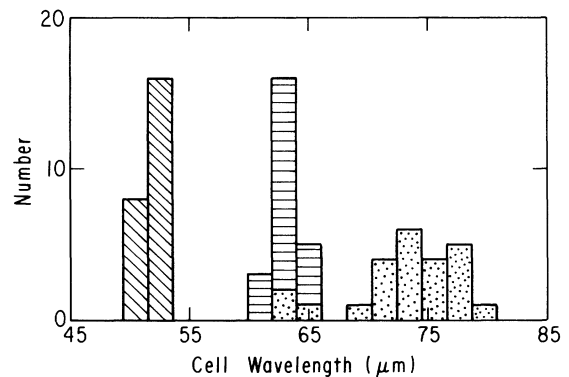


FIG. 3. Histogram of cell wavelength distributions. Bars shaded in dots, horizontal stripes, and diagonal stripes represent initial distribution at 40  $\mu\text{m}/\text{sec}$ , cells after the passage of one solitary mode, and cells after a quench from 100 to 40  $\mu\text{m}/\text{sec}$ , respectively.

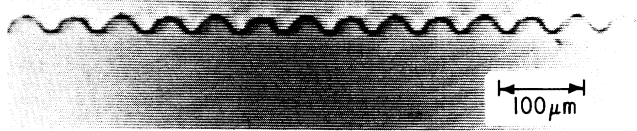


FIG. 4. A period-doubling cellular pattern, obtained after quenching the velocity from 100 to 40  $\mu\text{m}/\text{sec}$ .

locity within the solitary mode range (40  $\mu\text{m}/\text{sec}$ ), the interface will first come to a very uniform state of cells with  $\lambda < \lambda_s$  (Fig. 3). After about 2 min, we observe period doubling of the interface pattern (Fig. 4). We also occasionally observe higher-order modulations of the interface.

If instead of quenching the velocity to 40  $\mu\text{m}/\text{sec}$ , we quench it to 30  $\mu\text{m}/\text{sec}$ , the interface comes to the same compressed- $\lambda$  state and will, after 2 to 3 min, begin a series of amplitude oscillations (see Fig. 5). Each succeeding oscillation is larger and faster than the last, until the amplitude approaches 100% of the equilibrium cell amplitude where the largest swing in amplitude will collapse a cell. The fastest frequency is about 0.25 Hz, and there is an overall modulation of the amplitude. We believe that the long-wavelength amplitude modulations are manifestations of the Eckhaus instability. After the cell collapse, the overall wavelength is increased from  $52 \pm 2$  to  $63 \pm 2$   $\mu\text{m}$ , which is in the stability region.

To summarize, if we start from zero velocity and go to any  $v > v_s$ , we observe stable cells and moving defects. If we start from a larger velocity and reduce it to the same  $v$ , we impose a larger  $k$  vector. There is a critical  $k$ ,  $k_c$ , above which we always observe the Eckhaus instability. Period doubling appears only for a narrow range of  $k$  about  $k_c$ .

We note that the diffusion length in the isotropic phase at 40  $\mu\text{m}/\text{sec}$  is about 10  $\mu\text{m}$ , which is small compared to the cell wavelength (60  $\mu\text{m}$ ). Thus, local boundary-layer models of directional solidification may be useful.<sup>15</sup> In our system, the impurity diffusion constant in the nematic phase is about half its value in the isotropic phase ( $4 \times 10^{-6}$   $\text{cm}^2/\text{sec}$ ). Also, the partition coefficient  $k$  has a value of approximately 0.85 to 0.90. The thermal length  $l_T = m\Delta c/G$  is estimated to be about 50  $\mu\text{m}$ , while the capillary length  $l_C = (\gamma/L)(T_m/m\Delta c)$  is estimated from our experiment to be about 0.3  $\mu\text{m}$ . Here,  $m$  is the liquidus slope,  $\Delta c$  is the miscibility gap,  $G$  is the temperature gradient,  $T_m$  is the transition temperature of pure 8CB,  $L$  is the latent heat, and  $\gamma$  is the surface tension.

One approach to a theoretical understanding of the phenomena described above would be to write a Ginzburg-Landau equation for the order parameter (the amplitude of the cells).<sup>16</sup> The deduced phase equation is

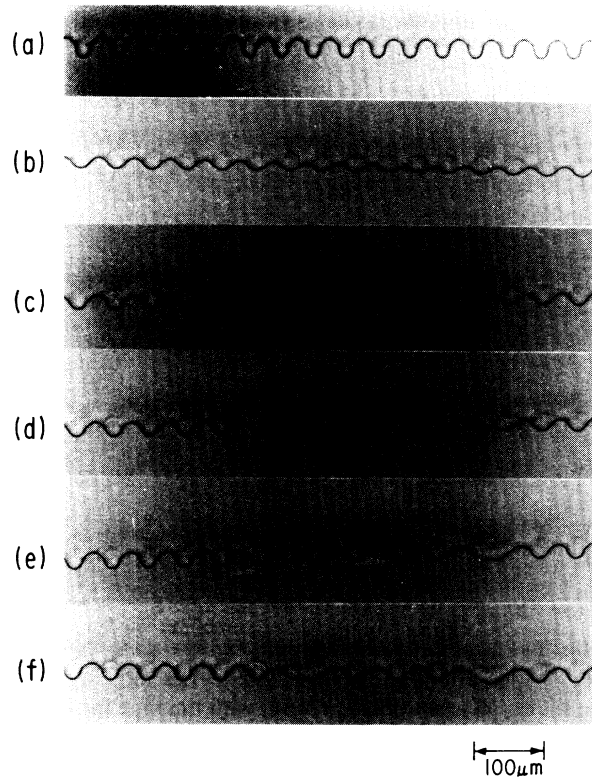


FIG. 5. Sequence showing the evolution of the interface after quenching from 100 to 30  $\mu\text{m}/\text{sec}$ . The time between each photo is approximately 0.5 sec. (a) The metastable state obtained immediately after quenching. (b) A long-wavelength, time-dependent, amplitude modulation. (c)-(f) The destruction of three cells because of the amplitude pulsation shown in (b).

known to have defect solutions and an Eckhaus instability.<sup>17</sup>

In conclusion, we have seen the solitary modes mediate pattern selection over a finite range of velocities. Our quenching experiments reveal the short-wavelength branch of the Eckhaus instability. As a corollary, we note that the wavelength of the system depends as much on the history of the solidification velocity as it does on the final velocity. Previous theoretical studies of directional solidification predict a band of stable wavelengths.<sup>18-21</sup> Their common feature was that they looked only at the stability of stationary solutions. We now have clear evidence that the selection mechanism is dynamic in the presence of solitary modes. For velocities below  $v_s$ , we see no sharp selection.

This work was supported by the Materials Research Laboratory under Grant No. DMR MRL 85-19460. One of us (J.B.) would like to thank AT&T Bell Laboratories for financial support.

<sup>1</sup>Patrick Oswald, John Bechhoefer, and Albert Libchaber,

Phys. Rev. Lett. **58**, 2318 (1987).

<sup>2</sup>W. W. Mullins and R. F. Sekerka, J. Appl. Phys. **35**, 444 (1965).

<sup>3</sup>J. S. Langer, Rev. Mod. Phys. **52**, 1 (1980).

<sup>4</sup>J. S. Langer, in *Chance and Matter*, Proceedings of the Les Houches Summer School, Session XLVI, edited by J. Souletie, J. Vannimenus, and R. Stora (Elsevier, Amsterdam, 1987).

<sup>5</sup>B. Caroli, C. Caroli, and B. Roulet, J. Phys. (Paris) **43**, 1767 (1982).

<sup>6</sup>Previous experiments in directional solidification have focused on the relation between cell or dendrite wavelength and velocity for the solid-liquid interface. See S. de Cheveigné, C. Guthmann, and M.-M. Lebrun, J. Phys. (Paris) **47**, 2095 (1986). Cf. R. Trivedi and K. Somboonsuk, Acta Metall. **33**, 1061 (1985), and also H. Esaka and W. Kurz, J. Crys. Growth **72**, 5 (1985).

<sup>7</sup>W. Eckhaus, *Studies in Nonlinear Stability Theory* (Springer-Verlag, Berlin, 1965).

<sup>8</sup>A. C. Newell and J. A. Whitehead, J. Fluid Mech. **38**, 279 (1969).

<sup>9</sup>G. Ahlers, D. S. Cannell, M. A. Dominguez-Lerma, and R. Heinrichs, Physica (Amsterdam) **23D**, 202 (1986).

<sup>10</sup>Mary Lowe and J. P. Gollub, Phys. Rev. Lett. **55**, 2575 (1985).

<sup>11</sup>Merck ZLI-3334.

<sup>12</sup>K. A. Jackson and J. D. Hunt, Trans. Metall. Soc. AIME **236**, 1929 (1966).

<sup>13</sup>John Bechhoefer, Ph.D. thesis, The University of Chicago, 1988 (unpublished).

<sup>14</sup>Similar effects, however, may be seen in the propagation of fronts. See G. T. Dee, Physica **15D**, 295 (1985) and G. T. Dee, J. Stat. Phys. **39**, 705 (1985).

<sup>15</sup>A. Karma and N. Goldenfeld, Phys. Rev. B **31**, 7108 (1985).

<sup>16</sup>P. Couillet, L. Gil, and J. Lega, to be published.

<sup>17</sup>General theoretical references that are relevant include G. Eilenberger, *Solitons: Mathematical Methods for Physicists* (Springer-Verlag, Berlin, 1983). On solitary modes as defects, see T. Kontorova and J. Frenkel, Zh. Eksp. Teor. Fiz. **8**, 89 (1938), and S. Aubry, in *Solitons and Condensed Matter Physics*, edited by A. R. Bishop and T. Schneider, Springer Series in Solid State Sciences, Vol. 8 (Springer-Verlag, Berlin, 1978), p. 264.

<sup>18</sup>A. Karma, Phys. Rev. A **34**, 4353 (1986).

<sup>19</sup>Thierry Dombre and Vincent Hakim, Phys. Rev. A **36**, 2811 (1987).

<sup>20</sup>M. Ben Amar and B. Moussalam, Phys. Rev. Lett. **60**, 317 (1988).

<sup>21</sup>D. Kessler and H. Levine, to be published.

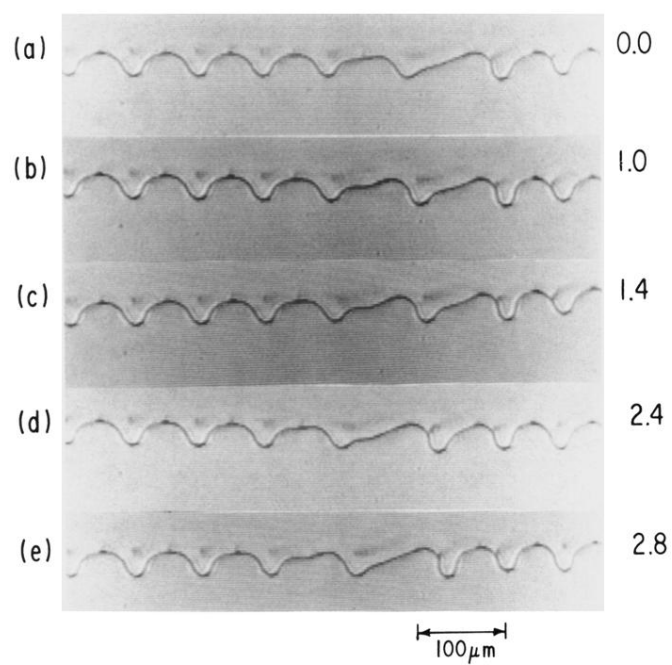


FIG. 1. Solitary mode propagating to the left. The sequence shows one cycle of the motion, with the time indicated, in seconds, on the right. Interface velocity =  $40 \mu\text{m}/\text{sec}$ .

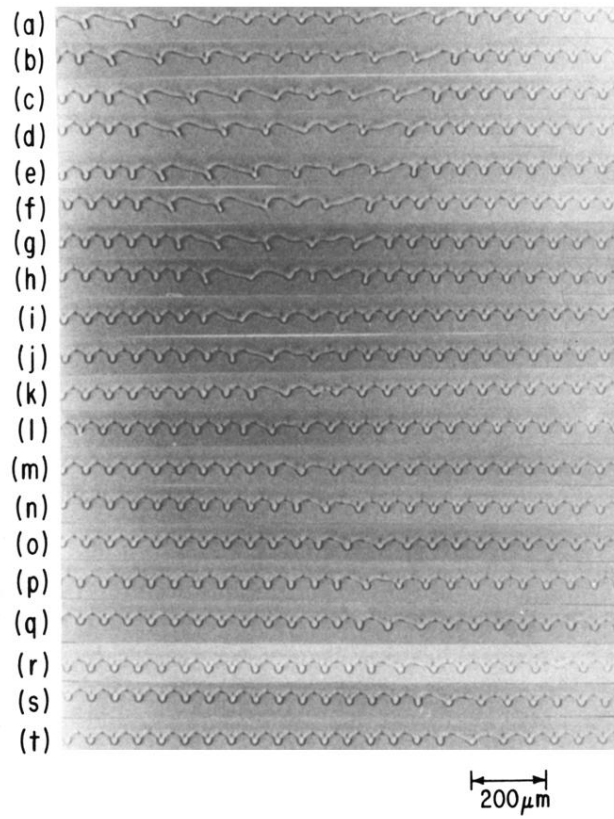


FIG. 2. Collision of two solitary modes. The result of the collision will be a single solitary mode propagating to the right. Velocity = 40  $\mu\text{m}/\text{sec}$ .

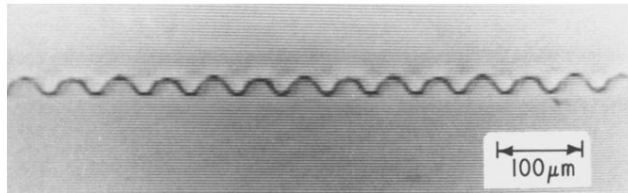


FIG. 4. A period-doubling cellular pattern, obtained after quenching the velocity from 100 to 40  $\mu\text{m}/\text{sec}$ .

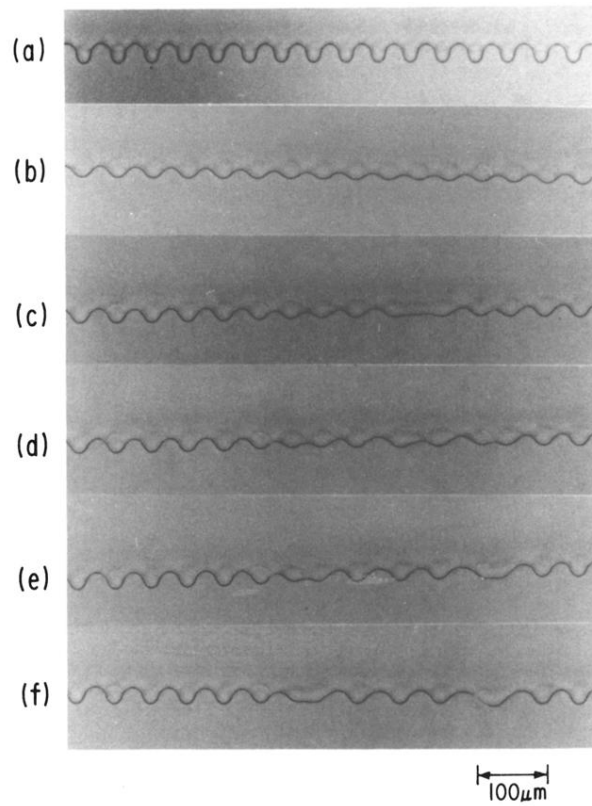


FIG. 5. Sequence showing the evolution of the interface after quenching from 100 to 30  $\mu\text{m}/\text{sec}$ . The time between each photo is approximately 0.5 sec. (a) The metastable state obtained immediately after quenching. (b) A long-wavelength, time-dependent, amplitude modulation. (c)–(f) The destruction of three cells because of the amplitude pulsation shown in (b).